Atmos. Chem. Phys. Discuss., https://doi.org/10.5194/acp-2017-482
Manuscript under review for journal Atmos. Chem. Phys.
Discussion started: 18 July 2017

Atmospheric Chemistry and Physics Discussions

Aerosol composition and the contribution of SOA formation over Mediterranean forests

Evelyn Freney[1], Karine Sellegri[1], Mounir Chrit[2], Kouji Adachi[3],Joel Brito[1], Antoine Waked[1]**, Agnès Borbon[1], Aurélie Colomb[1], Régis Dupuy[1], Jean-Marc Pichon[1], Laetitia Bouvier[1], Claire Delon[4], Corine Jambert[4], Pierre Durand[4], Thierry Bourianne[5], Cécile Gaimoz[6], Sylvain Triquet[6], Anaïs Féron[6], Matthias Beekmann[6], François Dulac[7], and Karine Sartelet[2]

[1]Laboratoire de Météorologie Physique, CNRS-Université Clermont Auvergne, UMR6016, 63117, Clermont Ferrand, France
[2]CEREA, Joint Laboratory École des Ponts ParisTech – EDF R & D, Université Paris-Est, 77455 Marne la Vallée, France
[3]Meteorological research institute, Atmospheric Environment and Applied Meteorology Research Department. 1-1 Nagamine, Tsukuba, Ibaraki 305-0052 Japan.
[4]Laboratoire d'Aérologie, CNRS-Université Paul Sabatier, Observatoire Midi-Pyrénées, Toulouse, France
[5]Centre National de Recherches Météorologiques, Météo-France-CNRS, Toulouse, URA1357, France
[6]Laboratoire Interuniversitaire des Systèmes Atmosphériques, LISA/IPSL, UMR CNRS 7583, Université Paris Est Créteil (UPEC) and Université Paris Diderot (UPD), France
[7]Laboratoire des Sciences du Climat et de l'Environnement, LSCE/IPSL, UMR 8212 CEA-CNRS-UVSQ, Université Paris-Saclay, Gif-sur-Yvette, France
**Now at IMT Lille Douai, Sciences de l'Atmosphère et Génie de l'Environnement (SAGE), F-59508 Douai Cedex, France/Université de Lille, F-59000 Lille, France

Correspondence to: *e.freney@opgc.univ-bpclermont.fr*

Abstract. As part of the Chemistry-Aerosol Mediterranean Experiment (ChArMEx), a series of aerosol and gas phase measurements were deployed aboard the SAFIRE ATR-42 research aircraft in summer 2014. The present study focuses on the 4 flights performed in late June early July over two forested regions in the south of France. We combine in situ observations and model simulations to aid in the understanding of secondary organic aerosol (SOA) formation over these forested areas in the Mediterranean and to highlight the role of different gas-phase precursors. The non-refractory particulate species measured by C-ToF-AMS instrument were dominated by organic species (60 to 72%) followed by a combined contribution of 25% by ammonia and sulphate aerosols. The contribution from the anthropogenic nitrate and black carbon (BC) concentrations, measured by an SP2, never contributed to more than 5% each to the total PM_1 mass concentration. Measurements of non-refractory species from off-line transmission electron microscopy (TEM) were coherent with the C-ToF-AMS instrument, showing a large contribution of externally mixed organic aerosol and externally mixed sulphate particles. Externally mixed organic aerosols, were equally identified with S signals, which may suggest the presence of organo-sulphates. Measurements of refractory species from TEM analysis showed a significant contribution of both sea salt and dust particles depending on the air mass trajectory. The organic aerosol measured by the C-ToF-AMS contained only evidence of oxidised organic aerosol (OOA), without a contribution of fresh primary organic aerosol. Positive matrix

Atmos. Chem. Phys. Discuss., https://doi.org/10.5194/acp-2017-482
Manuscript under review for journal Atmos. Chem. Phys.
Discussion started: 18 July 2017

factorization (PMF) on the combined organic/inorganic matrices separated the oxidised organic aerosol into a more oxidised organic aerosol (MOOA), and a less oxidised organic aerosol (LOOA). The MOOA component is associated with inorganics species and had higher O:C ratios than the LOOA factor. The LOOA factor is not associated with inorganic species and correlates well with biogenic volatile organic species measured with a PTR-MS, such as isoprene and its oxidation products (methylvinylketone (MVK), methacroleine (MACR), and isoprene hydroxyhydroperoxides (ISOPOOH)). Despite a significantly high mixing ratio of isoprene (2-4 ppbV) and oxidation products (0.6 and 1.2 ppbV), the contribution of specific signatures for isoprene epoxydiols SOA (IEPOX) within the aerosol organic mass spectrum (m/z 53 and m/z 82) were very weak, suggesting that isoprene SOA may be formed through a non-IEPOX route here, or with different precursors without clear mass spectral signatures in the C-ToF-AMS. This was corroborated through simulations performed with the Polyphemus model showing that 60 to 80% of SOA originated from biogenic precursors: about 15 to 32% isoprene (non-IEPOX) SOA, 10% sesquiterpenes SOA and 35 to 40% monoterpenes SOA). A total of 20 to 34% was attributed to purely anthropogenic precursors (aromatics and intermediate/semi volatile compounds).

1 Introduction

The contribution of anthropogenic aerosol particles is thought to be of the order of 10 Tg C yr^{-1}, however, that of natural biogenic aerosols has been estimated to be as much as 90 Tg C yr^{-1}, having an important effect on climate in both populated and remote areas of the world (IPCC, 2007, Hallquist et al. 2009). Our knowledge of how primary emissions from anthropogenic and natural sources contribute to the formation of secondary aerosols and their evolution in the atmosphere continues to improve with considerable advances in numerical simulations. However, discrepancies between simulations and measurements still exist and are more apparent over remote and forested environments than over anthropogenic environments (Ganzeveld et al. 2008; Lelieveld et al. 2008). The most commonly emitted biogenic volatile organic compounds (BVOCs) include isoprene and monoterpenes, with isoprene emissions accounting for approximately 44% (Kesselmeier and Staudt 1999; Arneth et al. 2008) . These species can be difficult to characterise because of their high temporal and spatial variability. Studies have shown that the formation yields of SOA from biogenic emissions alone is relatively low compared to those from anthropogenic souces, but when emissions from both biogenic and anthropogenic sources are combined the resulting yield for SOA formation is much higher than either anthropogenic or biogenic emissions alone (Day et al. 2009; Bryan et al. 2012; Shilling et al. 2013a; Hu et al., 2015).

The increasing improvement of instrumentation (namely aerosol mass spectrometry) available for the detection of different biogenic species, has led to an increase in the characterisation of biogenic SOA (BSOA). Several studies investigated BSOA in rural (Schwartz et al. 2010; Slowik et al. 2010; Ziemba et al. 2010; Setyan et al. 2014), Boreal (Kulmala et al., 2000; Allan et al., 2006), Amazonian (Martin et al., 2010), and some other tropical and subtropical forests (Capes et al. 2009; Robinson et al. 2011). Using aerosol mass spectrometry, a number of studies have identified specific signatures for isoprene derived SOA (Allan et al., 2014; Budisulistiorini et al., 2015). Hu et al., (2015) showed through comparison with model simulations,

that the global distribution of a particular SOA formation route from isoprene to epoxydiols is largely focused in the southern hemisphere and over Siberian forests far from anthropogenic emissions. The occurrence of these species in the northern hemisphere has been documented in several studies (Budisulistiorini et al., 2015), but in general the contribution is less than reported in the south hemisphere.

To our knowledge, no studies have identified SOA over the Mediterranean region. This region of Europe is thought to be extremely sensitive to climate change and is influenced by air masses from continental Europe, Northern Africa, as well as increasing emissions from biomass burning, intense shipping and from the increasing population density on Mediterranean coastal cities (e.g Sciare et al. 2003; Barnaba and Gobbi 2004; Lyamani et al. 2006; Alados-Arboledas et al. 2011; Mallet et al. 2013). Several studies have shown that during the summer months the aerosol radiative effect within the Mediterranean is one of the most significant in the world (Markowicz et al. 2002; Anton et al. 2012; Papadimas et al. 2012). Sartelet et al. (2012) modelled aerosol loading in Europe and North America, and retrieved high concentrations of ozone and SOA over the Mediterranean Sea. They estimated that biogenic emissions contributed to the formation of up to 72-88% of the SOA over Europe.

In the summer of 2014, the SAFMED (Secondary Aerosol Formation in the MEDiterranean) experiment took place in the Mediterranean as part of the Chemistry-Aerosol Mediterranean Experiment (ChArMEx; http://charmex.ipsl.lsce.fr). The main objective of the SAFMED experiment is to develop a better understanding of the sources of SOA over the Mediterranean region. A total of 14 research flights took place over the western Mediterranean region, with four of those flights being made over two different forested regions in the south of France, focusing specifically on biogenic emissions. In this work, we focus on the characterisation of aerosol chemical and physical properties and investigate the origin of SOA over these forested areas.

2 Methodology

2.1 ATR-42

All airborne measurements were preformed aboard the ATR-42, run by SAFIRE (French aircraft service for environmental research; http://www.safire.fr). The aircraft was based in Avignon, France. Aircraft flight plans were decided depending on forecasts from meteorological and air quality models made available on a dedicated operational web server called the ChArMEx Operation Centre (ChOC; http://choc.sedoo.fr). A series of different meteorological parameters were measured aboard the ATR-42 including temperature, pressure, relative humidity, turbulence, wind speed and direction as well as downward and upward radiances. In order to sample aerosol particle species, a forward facing aerosol inlet was fitted in place of a side window. This inlet is designed with an outer sleeve for chaneling air and a high tube radius of curvature to limit particle losses due to deposition. This inlet is both isokinetic and isoaxial and has a 50% sampling efficiency for aerosol particles with diameters of 4.5 µm (Crumeyrolle et al. 2013). From the aerosol inlet the sampled aerosols are orientated through a dispatcher to a number of different instruments.

Atmos. Chem. Phys. Discuss., https://doi.org/10.5194/acp-2017-482
Manuscript under review for journal Atmos. Chem. Phys.
Discussion started: 18 July 2017

Atmospheric Chemistry and Physics Discussions

2.2 Online aerosol chemical and physical properties

Aerosol particle number concentrations were measured using a scanning particle mobility sizer (SMPS) with 162 size channels for particle diameters ranging from 20 nm up to 400 nm. Larger particles size distributions were measured using a GRIMM optical particle counter with 16 size channels from 265 nm up to 3 microns. Measurements of aerosol chemical properties were performed using a compact aerosol time of flight mass spectrometer (C-ToF-AMS). This instrument was operating with a time resolution of 40 seconds in order to ensure that the maximum amount of temporal information could be obtained on aerosol properties while ensuring a high enough signal to noise ratio. Prior to being sampled into the C-ToF-AMS, aerosol particles passed through a pressure controlled inlet (PCI). This inlet maintained a constant pressure of about 400 hPa throughout the duration of the flight and ensured that there were no changes to inlet pressure during in-flight sampling (Bahreini et al., 2008). In order to provide quantitative information on aerosol mass concentrations, a collection efficiency (CE) must be applied to the aerosol mass concentrations. This is based on the principle that the C-ToF-AMS aerodynamic inlet is designed to sample dry spherical particles and that particles with non-spherical shapes will not be as efficiently sampled. In addition to this sampled aerosols particles can sometimes be lost in the instrument as a result of particle bounce on the heating filament. This CE correction is chemical dependant (Middlebrook et al., 2012). Since the contribution of nitrate and sulphate remained lower than 25%, the CE remained at 50% throughout the sampling period. The total mass measured by the C-ToF-AMS (combined with that from the BC measurements) was compared to the total aerosol concentration measured by the SMPS set up (Fig. S1). All reported concentrations are in standard temperature and pressure.

2.3 Gas-phase measurements

Gas-phase species were sampled aboard through a rear facing ¼ inch Teflon tube. Ozone and CO were measured using ultra-violet and infra-red analysers (Thermo-environmental instruments) (Nedelec et al. 2003). The NO and NO_X measurements were performed using an ozone chemiluminescence instrument (Environment SA AC42S instrument). The quantification of NO_2 is obtained from converting into NO using a molybdenum converter at 320 °C. As also some NO_Y is converted into NO in the molybdenum oven, the NO_2 and NOx concentration can be overestimated. In this work, these measurements will be referred to as NO_W, and refers to NO + NO_2 + an unquantified NOy. Formaldehyde concentrations were measured every 30 s using an Aerolaser 4021 instrument. Full details of the operation of the Aerolaser instrument are provided in Waked et al., (this special issue). For measurements of volatile organic compounds, a high sensitivity proton-transfer-reaction mass spectrometer (PTR-MS) from Ionicon Analytik (Innsbruck, Austria) was used, with a time resolution of 19s. Full details of the PTR-MS configuration on-board and operating conditions are provided in Borbon et al. (2013). During the so-called biogenic flights, 16 protonated masses were monitored. Compounds of interest are:

- VOCs of biogenic origin and their first generation oxidation products (BVOCs) including m/z 69 (isoprene), m/z 71 (sum of methylvinylketone (MVK) and methacroleine (MACR) and isoprene hydroxyhydroperoxides (ISOPOOH)), m/z 137 (sum of monoterpenes);

- anthropogenic volatile organic compounds (AVOCs) including m/z 79 (benzene), m/z 93 (toluene), m/z 107 (C8-aromatics), and m/z 121 (C9-aromatics);
- oxygenated VOCs (OVOCs) including m/z 33 (methanol), m/z 45 (acetaldehyde), and m/z 59 (acetone).

Detection limits, defined as 3σ in background mixing ratios ranged from 0.05 ppb to 2.70 ppb over a 1s dwell time. Instrumental background signal was determined through periodic air sampling (triplicates) of ambient air scrubbed through a custom-built catalyst converter (platinum-coated steel wool) heated to 250ºC. Three complete calibrations over a 0.1-20 ppb range were performed before, during, and after the campaign. The standard gas used was provided by Ionimed (Innsbruck, Austria) and contained several VOCs including isoprene, α-pinene, benzene, toluene and o-xylene at 1 ppm certified at ±5%. A second ppb-level gaseous standard from NPL (UK) was used to cross-check the quality of the calibration and to perform regular one-point calibration control for isoprene and C6-C9 aromatics (4 ± 0.8 ppb). A relative difference of less than 10% was found. The calibration factor for all major VOCs (the slope of the mixing ratio with respect to product ion signal normalized to H_3O^+) ranged from 2.35 (m/z 137) to 18.9 (m/z 59) counts sec^{-1}.

2.4 Statistical analysis

Detailed analysis of the organic aerosol mass spectra measured by the C-ToF-MS was performed using positive matrix factorization (PMF) (Paatero,1997). The PMF2 software package (P.Paatero, University of Helsinki, Finland) was used in conjunction with the PMF analysis and evaluation tool (Version 2.04; Ulbrich et al., 2009). Recommended procedures of downweighting for certain m/z values were followed (Ulbrich et al., 2009) as well as removal of several m/z values due to low (m/z 19 and 20) or high signal (m/z 29). In this particular case, m/z values from inorganic ions (SO_4, NO_3) were equally combined with the organic matrices to better separate different factors. Error values for all m/z were calculated in the same way using squirrel software (version 1.53) and adjusted using the recommendations of Paatero and Hopke (2003). The number of factors was determined using correlations with external factors (temporal series of VOCs measurements). The reported correlations used later on in the discussion were calculated using simple linear regression.

2.5 Electron microscopy analysis

Aerosol particles were collected on transmission electron microscope (TEM) grids using a sampler consisting of two impactor stages. The 50% cut-off of each of these stages was calculated to be 1.6 µm and 0.2 µm respectively, with a flow rate of approximately 1.0 L min^{-1}. The samples were collected only when the aircraft was traveling at a constant altitude, usually lasting between 15 and 20 minutes. These TEM grids were then analysed using a 120 kV TEM (JEM-1400, JEOL) to provide detailed information on individual aerosol compositions and shapes. The advantage of having TEM analysis is that we are able to detect refractory and non-refractory aerosol particles. Composition of each sample collected was analysed using energy-dispersive X-ray spectrometer (EDS) with scanning-TEM mode (Adachi et al., 2014). There were at least 50 particles analysed from each grid. Particles were classified into five aerosol categories based on their compositions: organic

aerosol (C dominant), sulphate (S dominant), sulphate + organic (C and S dominant), sea salt (Na dominant), and other (e.g., mineral dust (Si dominant, but also included traces of Ca and K)).

2.6 Back trajectory analysis

In order to determine the history of air masses prior to being sampled by the aircraft, air mass trajectories were calculated for a 24-hour period using the Lagrangian model HYSPLIT (http://ready.arl.noaa.gov/HYSPLIT.php). These air mass trajectories were calculated for intervals of five minutes along the flight track and provide information on the dominant air mass sources during the flight. Back trajectories of 24 hours provided enough information to determine whether air masses were slow moving and local, or fast moving and arriving over larger distances (Fig. S2). For all flights, the air mass trajectory path was constant along the flight track at low altitudes, showing that air masses of the same origin were measured during each flight. 72-h back trajectories were also computed (although not shown) in order to determine possible aerosol sources over longer time scales.

3 Results

3.1 Overview of flights

Four research flights (RF) dedicated to biogenic emissions studies were carried out, taking place between the 30th of June (RF15) and 7th July 2014 (RF23). Each flight was approximately 3.5 hours in duration, and the aircraft flew over forested areas with elevations varying from 250 to 500 m above ground level (a.g.l) during straight and level runs. The flight plan consisted of the aircraft leaving the city of Avignon (southern France) and travelling east/west for about 50 km before starting a vertical sounding. Vertical soundings were performed from around 100 up to 3000 m above sea level (a.s.l). Using the vertical profiles of VOC concentrations and relative humidity, the atmospheric boundary layer height was determined for each flight, and varied from 1300 m a.s.l (RF20 03/07) up to 1900 m a.s.l (RF15 30/06) (Fig. S4). Two of the flights (RF15 30/06, RF21 05/07) flew west over the Puéchabon Mediterranean national forest region (North-West of Montpellier, Fig. S5a), where the principle type of vegetation is evergreen oaks (Quercus ilex) and Alpine pines (halepensis). The evergreen oak is not an isoprene-emitting species; it is known to emit several different types of monoterpene species but mainly α-pinene (Loreto et al., 1996). The other two flights (RF 03/07 RF20, RF 07/07 RF23) flew east over the Oak Observatory field site at Observatoire de Haute Provence (O3HP, https://o3hp.obs-hp.fr, Fig. S5b). This area is dominated by downy oak trees (Quercus pubescens) but also contains Montpellier maple (Acer monspessulanum) and smokey bushes (Cotinus coggygria) in a lower canopy stage. Since Quercus pubescens is the dominant type of vegetation, it makes this region a strong isoprene emitting region and an ideal area to study isoprene chemistry and its relation to aerosol particles (Zannoni et al., 2015).

For the flight RF20 03/07, temperatures were stable, varying from 18 to 19^{o}C in the boundary layer, and wind speeds were always less than 5 ± 1 m s^{-1}, originating from a south-easterly direction. HYSPLIT air mass back trajectories show that for a

24-hour period prior to the measurements, air masses were slow moving and remained within a 200 km radius of the sampling site (Fig. S2b). This, together with the clear skies and relatively high temperatures made ideal conditions to study local biogenic emissions. RF23 07/07, had similar temperatures to those recorded on RF20 03/07 (17 to 20°C), but with some cloud cover. Wind speeds ranged between 2 and 4 m s^{-1}, air masses arrived from a southerly direction passing over the coast line prior to being sampled along the flight track (Fig. S2d). For the two westerly flights, average temperatures were slightly higher 23 ±1 °C. Wind speeds were low, (3 ± 1 ms^{-1}). Air masses travelled much greater distances over western (RF15 30/06) and northern (RF21 05/07) parts of France prior to being sampled (Fig. S2, a, c).

3.2 Gas-phase properties

The principal VOC species measured by the PTRMS during all flights were acetone (m/z 59) and methanol (m/z 33), followed by isoprene (m/z 69) and its oxidation products (MVK + MCR + ISOPOOH) (m/z 71) and then VOC species representative of monoterpenes emissions (m/z 137). Anthropogenic VOC species (m/z 93 (toluene), m/z 79 (benzene), and aromatics) never contributed more than 5% to the total VOC measured (Table 1, Fig. 1).

Using OH reactivity, the contribution of VOC species to photochemical activity was evaluated. This was calculated for each of the measured species using the method described by Atkinson and Arey, (2003), full details are provided in Waked et al., (this special issue). OH reactivity promotes the formation of secondary species such as formaldehyde (HCHO) and O_3. The results obtained for many VOC's and OVOC's showed that isoprene is the main reactant with OH for the biogenic flights (RF30/06 to RF07/07) with a contribution ranging from 46-57% followed by formaldehyde (12-29%) and acetaldehyde (7-21%) (Fig A6). Therefore, these compounds (isoprene, formaldehyde and acetaldehyde) explain at least more than 83% of the total identified OH reactivity. Detailed discussion of the origins and evolutions of gas-phase species during the SAFMED project is provided in a separate manuscript within this issue (Waked et al, this special issue).

3.3 Aerosol chemical properties

For all flights, aerosol composition measured by the C-ToF-AMS instrument shows that the organic compounds contributed a significant fraction to the total aerosol concentration during all flights (with average values of 72 (± 36) % for RF20 03/07 and 71 (± 30) % for RF23 07/07) (Table 2, Fig. 2). The second most dominant species measured were sulphate and ammonium aerosol particles, with a combined contribution of up to 25 ± 10%. The contribution from nitrate species was on average 3 (± 1.5)%. Black carbon (BC) measured using the SP2, never exceeded 5% to the total PM1 mass (Fig. 2). The organic aerosol measured during all flights was well oxidised, having average O:C ratios of 0.89 (± 0.18), with little evidence of fresh primary organic aerosol.

TEM measurements showed that at least 35 (± 5) % of all aerosol particles measured was made up of externally mixed organic aerosol, 15 (± 5) % was externally mixed sulphate particles and 10 % were internally mixed organic and sulphate (likely ammonium sulphate) species (Fig. S7). The high contribution of externally mixed particles indicates that most of aerosol particles were recently emitted from their source and did not have sufficient time for mixing with other species prior

to sampling. The remaining fractions were made up of sea-salt and dust particles. Only considering the non-refractory fractions measured by the TEM, we observe that organic, sulphate, and internally mixed particles contributed approximately 60%, 25%, and 15%, respectively, similar to C-ToF-AMS observations. Sea-salt aerosol particles contributed 15% to the submicron number concentration of the aerosol particles measured during RF20 03/07, and less than 5% for the other flights. Air mass trajectories calculated over a 72hr period, show that for RF20 air masses arrived from over the Mediterranean, which would explain the contribution from marine aerosol particles. Also shorter time circulations like daily sea-breezes could be invoked to explain sea-salt presence in the flight area. The remaining particles were classified as "dust particles" and contained traces of Si, Na, Ca, and Si + S-rich particles with geometric diameters of several µm. TEM analysis of aerosols collected during RF23 07/07 shows the "dust" category contributing up to 40% to the measured aerosol, suggesting that there was a relatively strong influence from dust emissions during this flight. The Si + S particles probably reveal internally mixed particles following reactions of acidic sulphur species with basic species such as $CaCO_3$ present in soil dust (Loÿe-Pilot et al., 1986; Manktelow et al., 2010). Investigating the externally mixed organic aerosol in more detail, it was observed using EDS mapping techniques that these amorphous organic aerosol particles contained signals for sulphur (Fig. 3). These S signals were detected within the amorphous organic particle, but showed no visual evidence of other particulate matter or compounds e.g. ammonium sulphate (Fig A7). From these measurements we could conclude that the S was part of the molecular structure of the organic compound, possibly in the form of organo-sulphates.

3.4 Aerosol physical properties

Aerosol size distributions measured using the SMPS during the four biogenic flights are illustrated in Fig. 4. During the westerly flight RF15 30/06, when air masses were travelling from the north west of France, particle concentrations were on average 1500 ± 300 cm^{-3} and the principle size mode was less than 90 nm at altitudes of around 500 m. At higher altitudes aerosol number concentration decreased to 600 ± 200 cm^{-3}, and with modal diameters of around 30 ± 20 nm (Fig. 4a). The measured particle concentrations during the other westerly flight RF21 05/07 were on average 1895 ± 1707 cm^{-3}. The fraction of fine particles, < 40 nm in diameter (F40) measured during these flights was high; explaining the lower aerosol mass measured using the C-ToF-AMS instrument. During the two easterly flights, average aerosol number concentrations were considerably higher at 3332 ± 1920 cm^{-3} (Fig. 4b and d). The size distribution of the aerosol had a single mode at around 100 nm. However, during periods with increased aerosol concentrations, the size distribution spectra showed an additional mode between 20 and 40 nm. These higher particle concentrations and larger diameters ($F40 < 0.3$) explain why the total mass measured by the C-ToF-AMS is much higher for the easterly experiments rather than the westerly experiments.

The increases in fine mode particles measured at lower altitudes (~500 m. a. g.l) during all flights are likely linked to new particle formation. Observations of new particle formation from biogenic emissions have been reported over Boreal forests (Sihto et al. 2006), European coniferous forests (Held et al. 2004), African savannah forests (Laakso et al. 2013), as well as during laboratory studies (Kiendler-Scharr et al. 2009). Monoterpenes oxidation products were shown to produce new

particles by nucleation more efficiently than the isoprene oxidation products (Spracklen et al., 2008; Bonn et al. 2014). Some of these studies have also shown that high concentrations of isoprene relative to monoterpenes can inhibit new particle formation (Kiendler-Scharr et al. 2009; Kanawade et al., 2011), although the underlying processes are not yet clear. Using the measurements available during these four flights, we investigated this relationship between biogenic VOC species and new particle formation; we calculated the ratio of isopreneC/monoterpeneC and compared it with F40. This ratio of isopreneC/monoterpeneC varied between 0.05 and 8 (average 3 ± 1), with lowest values corresponding to highest fractions of fine particle concentrations (Fig. 5). These observations are in agreement with previous field studies over mixed deciduous forests (Kanawade et al., 2011) and with laboratory studies in controlled environments showing that high concentrations of monoterpenes, relative to isoprene, can favor new particle formation (Kiendler-Scharr et al., 2009). The average ratios of isopreneC/monoterpeneC measured during these Mediterranean flights were higher than the ones reported within Finnish forests (ratios of 0.18) and lower than the ones measured in Michigan (rations of 26.4) and Amazonian forests (ratios of 15.2) (Kanawade et al., 2011. In general, higher ratios are associated with very little or suppressed new particle formation events.

3.4.1 Secondary organic aerosol

From C-ToF-AMS measurements average mass concentrations measured during the two easterly flights was approximately 2.0 ± 0.5 μg m^{-3}, whereas that measured by the westerly flights was considerably less at approximately 1 μg m^{-3}, making more detailed analysis of aerosol chemical properties difficult. For this reason the remaining analysis is focused on the two easterly flights.

For both easterly flights, increases in organic aerosol concentrations were observed in the valley area between the two higher elevation areas (between 43.6 and 43.8°N) during horizontal transects of the flight. For RF20 03/07, these increases were accompanied by significant increases in the fine particulate matter between 20 and 40 nm, and also those at 90 nm. In addition, increases in the ratio of isoprene oxidation products to isoprene were observed in the same region, implying a more oxidised air mass. A time series plot of total organic aerosol (OA) with MCR+MVK+ISOPOOH shows a good relationship (Fig. S8a) and plotting OA against the ratio of (MCR+MVK+ISOPOOH)/isoprene as a proxy for the photochemical age, we observe a reasonable correlation (r = 0.46) and positive slope (b = 1.1) with increasing OA as photochemical age increases, suggesting the formation of SOA from isoprene originating biogenic precursors (Fig. S8 b).

In order to extract additional information on the OA measured during the flights, we combined the organic and inorganic mass spectra and performed PMF analysis. For both flights; a two-factor solution (f-peak 0) was chosen to best describe the sources of the aerosol particles and those 2 factors have maximum correlations with external species (Table 3). They include (i) a more oxidised organic aerosol (MOOA, contributing 55%), containing high contributions from m/z 44 and associated with inorganic peaks (m/z 30, 46 (NO_3), and 48, 64, 80 (SO_4)) and (ii) a less oxidised organic aerosol species (LOOA, contributing 45%) with little contribution from inorganic m/z (Fig. 6 a)). These two factors MOOA and LOOA are very similar to the OOA-1 and OOA-2 species identified from ground-based measurements during a biogenic event over a

forested area in Canada (Slowik et al. 2010). Slowik et al., (2010) showed similar trends with the two identified oxidised organic aerosol, where one was associated with inorganic aerosols and the other was not correlated with inorganic aerosols but was well correlated with biogenic VOC species. Plotting these two species as a function of the photochemical age we observe a significant increase of the LOOA species with increasing ratios (MCR+MVK+ISOPOOH/Isoprene) until a maximum is reached at ratios of 0.65. Interestingly MOOA remains relatively stable, indicating an independent source.

We observe that isoprene and its oxidation products are better correlated with the LOOA than with MOOA. Several recent publications have identified signature peaks in aerosol mass spectrometry for isoprene derived SOA, using the m/z 53 and m/z 82 (ionisation products of IEPOX) (Allan et al., 2014, Budisulistiorini et al, 2015, Zhang et al., 2017). In this study, the contribution of these peaks in both types of spectra was very low (fraction of signal < 0.004), although somewhat more pronounced for LOOA. These contributions are similar to background contributions of f82 observed globally by Hu et al., (2015), ranging from 0.0002 and 0.0035, and would lead us to believe that we have no significant contributions of f82 in our aerosol mass spectra. These low values of f82 are similar to those from studies investigating biogenic SOA influenced by monoterpenes emissions, for example Hu et al. (2015).

Formation routes of isoprene SOA, that do not follow the IEPOX route have been observed and have been suggested to contribute to m/z 91 in the AMS mass spectral signatures (Krechmer et al. 2015; Riva et al., 2016). This m/z 91 was present in all OA mass spectra and was significantly higher for the LOOA than for the MOOA. In recent work, on the characterisation of aerosol particles over coniferous forests (mainly monoterpenes emitters) this has been shown to be due to the $C_7H_7^+$ fragment (Lee et al., 2016). It should be noted that m/z 91 can also be associated with fragments of primary OA and therefore other potential sources cannot be excluded.

Factors influencing the formation of isoprene SOA include aerosol acidity and the presence of NO_X and sulphate (Nguyen et al., 2014, Xu et al., 2015), with highest yields of isoprene SOA being measured under low-NO_X conditions (<30 pptV) and in the presence of acidic aerosols (Gaston et al., 2014). There have been some reports of isoprene-derived SOA formation (hereafter isoprene SOA) in high-NO regions but the contribution of this pathway is considered to be much smaller (Jacobs et al., 2014). NO_W concentrations measured during these flights varied from 6 up to 10 ppbV, however the average concentrations of NO are 0.30 ± 0.2 ppbV, suggesting that the real contributions of NO_X (See section 2.3) is also likely to be low. Absolute concentrations of isoprene during these flights varied from 500 up to 1800 pptV. There have recently been an increasing number of studies showing either IEPOX can be formed from combined anthropogenic and biogenic processes or that the formation pathways of IEPOX need to be revisited (Zhang et al, 2017). Under low-NOx regimes, isoprene SOA may be formed from other routes than IEPOX, such as hydroperoxides (Krechmer et al. 2015; Riva et al., 2016). Other forms of isoprene SOA from oxidation by NO/NO_2 are methacrylic acid epoxide (Worton et al., 2013), however the formation yields associated with these reactions are much lower than those associated with IEPOX. Using gas-phase measurements, we observe that isoprene was the main contributor to the photochemical activity during these biogenic flights (Fig. S6) and given the significant correlation with isoprene and its oxidation products but the lack of isoprene SOA signatures (m/z 82), we can conclude that the observed OA can probably be related to a non-IEPOX isoprene SOA.

Atmos. Chem. Phys. Discuss., https://doi.org/10.5194/acp-2017-482
Manuscript under review for journal Atmos. Chem. Phys.
Discussion started: 18 July 2017

Atmospheric Chemistry and Physics Discussions

3.4.2 Model evaluation of secondary organic aerosol formation

In order to examine in more detail the relative contribution of the different gaseous precursors on SOA formation over these forested flights, two simulations were performed using the Polyphemus model. Full details of the model set up are available in Chrit et al., (this special issue). The domain of the air-quality simulation has an horizontal resolution of 0.125° x 0.125°, while the vertical is modelled with 14 layers having interface heights at 0, 30, 60, 100, 150, 200, 300, 500, 750, 1000, 1500, 2400, 3500, 6000, 12000 m. above sea level (asl) (Fig. S3). Biogenic emissions are computed using MEGAN (Guenther et al. 2006), and anthropogenic emissions using HTAP-v2 (http://edgar.jrc.ec.europa.eu/htap_v2/). Initial and boundary conditions are obtained from a larger-scale simulation (over Europe), as detailed in Chrit et al. (this special issue). For gaseous chemistry, the model used is a carbon bound approach (CB05; Yarwood et al., 2005). Aerosol dynamics is modelled with a sectional approach (SIREAM; Debry et al., 2007), and for SOA modelling, a surrogate approach is used (Couvidat et al. 2012). Biogenic precursors are isoprene, monoterpenes (with α-pinene and limonene as surrogates) and sesquiterpenes, with low-NOx and high NOx oxidation regimes. Isoprene may form two surrogates, amongst which methylmethyl dihydroxy dihydroperoxide under low NOx, and methyl glyceric acids under high NOx. Monoterpenes may form pinonaldehyde, norpinic acid, pinic acid, 3-methyl-1, 2, 3-butanetricarboxylic acid (MBTCA) under low-NOx, and organic nitrate, as well as extremely low volatile organic carbons (ELVOCs) or highly oxidized multifunctional organic compounds (HOM) by ozonolysis. Anthropogenic precursors are toluene, xylene and intermediate/semi volatile organic compounds (I/SVOC). Emissions of I/SVOC are estimated by multiplying emissions of primary organic aerosols by a factor 2.5 (Zhu et al. 2016). Partitioning between the gas and aerosol phases is done with secondary organic aerosol processor model (SOAP) (Couvidat and Sartelet, 2015) for organics and inorganic aerosol model ISORROPIA for inorganics (Nenes et al. 1998).Maps of the simulated submicron organic matter (OA_1) are shown in Figure A3a and A3b for the two easterly flights RF20 03/07 and RF23 07/07 flights, respectively.

Figure 7 compares the vertical profiles of measured and modelled OA_1 during the RF20 03/07 and the RF23 07/07 flights. The concentrations averaged over the vertical layers of the model and the standard deviations around the mean concentrations are shown. The measured concentrations have higher standard deviations than the modelled concentrations, due to the coarse horizontal model resolution (0.125° x 0.125°). For RF23 07/07, the modelled mean concentrations for OA_1 is underestimated in the vertical layer between 300m and 500m (1.0 µg m^{-3} measured and 0.6 µg m^{-3} modelled), and over-estimates the measurements between 500m and 750m (0.45 µg m^{-3} measured and 0.7 µg m^{-3} modelled). However, this discrepancy may be due to difficulties in representing the vertical distribution of pollutants above the canopy. Although the mean vertical concentrations of OA_1 tends to be under-estimated over 1000 m, they are on average well modelled under 1000m within the boundary layer for both flights (1.3 µg m^{-3} measured and 1.3 µg m^{-3} simulated for RF20 03/07; 0.8 µg m^{-3} measured and 0.7 µg m^{-3} simulated for RF23 07/07).

Figure 8 shows the modelled composition of the OA_1 along the flight path for RF20 03/07 and the RF23 07/07 flights. Although isoprene emissions are much higher than those of monoterpenes and sesquiterpenes over that region, isoprene-

derived SOA represent only about 15 to 35% of the simulated OA, while monoterpenes-derived SOA represent 35% to 40%: 4% to 7% are from semi-volatile organic compounds (pinic acid, norpinic acid and pinonaldehyde), 9% to 14% from ELVOCs/HOMS, and 17% to 23% from organic nitrate. Sesquiterpenes derived OA represent about 10%. In total, biogenic-derived OA represents about 66% to 80% of OA. The rest is made up by aromatics derived OA (2% to 3%) and anthropogenic intermediate and semi volatile organic compounds (17% to 31%). The measured organic matter is highly oxidized during both flights with an average measured ratio O/C below 1000m of 1.05 during the RF20 03/07 flight and 1.1 during the RF23 07/07 flight. This ratio is very well represented by the model with an average values of 1.07 (RF20 03/07) and 1.17 (RF23 07/07). In the model, these high O/C ratios arise because of organic compounds from isoprene oxidation, which all have O/C ratio greater than 0.8, as well as some ELVOCs compounds (monomers) from monoterpenes oxidation.

The model estimates a significant contribution of isoprene SOA (approximately 15 to 35% to the total SOA). This cannot be confirmed by measurements due to the lack in a significant contribution of m/z 82 in the AMS spectra.

4 Conclusion

This paper characterises aerosol and gas-phase physical and chemical properties over two different forested areas in southern France. During four dedicated flights, aerosol particle, and gas-phase composition were measured using a C-ToF-AMS and a PTR-MS, with the principle objective to characterise biogenic emissions. Aerosol particle physical properties were measured using a number of different techniques characterising particle size and number concentrations. Using a combination of aerosol size distributions coupled with VOC concentrations we observe that although new particle formation seem to occur over all types of vegetation (mainly isoprene-emitting species or mainly monoterpene-emitting species), that high isopreneC/monoterpeneC ratio can favour the formation of fine aerosol particles. These VOC species are likely condensing on newly formed particles and on pre-existing particles that can then be chemically analysed.

During eastern flights, in valley areas, high concentrations of organic aerosol and biogenic VOC species were measured (isoprene and its oxidation products MCR+MVK+ISOPOOH). PMF analysis on the organic mass spectra separated two organic factors namely a more oxidised organic aerosol (MOOA) and a less oxidised organic aerosol (LOOA). The MOOA species were strongly associated with SO_4 species whereas the LOOA species were not related to inorganic species but correlated with the total concentrations of isoprene oxidation products (MCR+MVK+ISOPOOH). However, the lack of direct evidence of IEPOX-SOA (mz 82 $C_5H_6O^+$) it is thought that IEPOX-SOA may have reacted to form organosulfates or that the SOA may be linked to other routes of isoprene SOA formation or/and other biogenic and anthropogenic precursors. Although the measured isoprene emissions dominate over the measured monoterpene emissions in the region, simulated SOA is only made of 15% to 35% isoprene SOA, the remaining modelled SOA is attributed to monoterpenes (35% to 40%)

and sesquiterpenes (10%) precursors. The combination of both observations and numerical models show the importance of non IEPOX formation routes to the formation of biogenic SOA.

Acknowledgments

This study received financial support from MISTRALS by ADEME, CEA, INSU, and Meteo-France. This research was also funded by the SAFMED (Secondary aerosol formation in the Mediterranean) (ANR, grant number: ANR-12-BS06-0013-2502). The authors would also like to extend a special thanks to the pilots and flight crew from SAFIRE for all their enthusiasm and support during the measurement campaign aboard the ATR-42 aircraft. In addition, the authors are very grateful to Eric Hamonou for his logistical help in organizing the campaign, and to Laurence Fleury, Hélène Ferré and the OMP/SEDOO team who provided excellent support to aircraft operations through the ChOC web interface setup and management.

References

Adachi, K., Zaizen, Y., Kajino, M., and Igarashi, Y.: Mixing state of regionally transported soot particles and the coating effect on their size and shape at a mountain site in Japan, J. Geophys. Res. Atmos., 119, 5386–5396, doi:10.1002/2013JD020880, 2014.

Atkinson, R., and Arey, J.: Atmospheric degradation of volatile organic compounds, Chem. Rev., 103, 4605–4638, doi:10.1021/cr0206420, 2003.

Alados-Arboledas, L., Müller, D., Guerrero-Rascado, J. L., Navas-Guzmán, F., Pérez-Ramírez, D., and F. J. Olmo, F.J.: Optical and microphysical properties of fresh biomass burning aerosol retrieved by Raman lidar, and star-and sun-photometry, Geophys. Res. Lett., 38, L01807, doi:10.1029/2010GL045999, 2011.

Allan, J. D., Alfarra, M. R., Bower, K. N., Coe, H., Jayne, J. T., Worsnop, D. R., Aalto, P. P., Kulmala, M., Hyötyläinen, T., Cavalli, F., and Laaksonen, A.: Size and composition measurements of background aerosol and new particle growth in a Finnish forest during QUEST 2 using an Aerodyne Aerosol Mass Spectrometer, Atmos. Chem. Phys., 6, 315-327, doi:10.5194/acp-6-315-2006, 2006.

Allan, J. D., Morgan, W. T., Darbyshire, E., Flynn, M. J., Williams, P. I., Oram, D. E., Artaxo, P., Brito, J., Lee, J. D., and Coe, H.: Airborne observations of IEPOX-derived isoprene SOA in the Amazon during SAMBBA, Atmos. Chem. Phys., 14, 11393–11407, doi:10.5194/acp-14-11393-2014, 2014.

Antón, M., Valenzuela, A., Román, R., Lyamani, H., Krotkov, N., Arola, A., Olmo, F. J., and Alados-Arboledas, L.: Influence of desert dust intrusions on ground-based and satellite-derived ultraviolet irradiance in southeastern Spain, J. Geophys. Res. Atmos., 117, D19209, doi:10.1029/2012JD018056, 2012.

Arneth, A., Monson, R. K., Schurgers, G., Niinemets, Ü., and Palmer, P. I.: Why are estimates of global terrestrial isoprene emissions so similar (and why is this not so for monoterpenes)?, Atmos. Chem. Phys., 8, 4605-4620, doi:10.5194/acp-8-4605-2008, 2008.

Bahreini, R., Dunlea, E. J., Matthew, B. M., Simons, C., Docherty, K. S., DeCarlo, P. F., Jimenez, J. L., Brock, C. A., and Middlebrook, A. M.: Design and operation of a pressure-controlled inlet for airborne sampling with an aerodynamic aerosol lens, Aerosol Sci. Technol., 42, 465–471, doi:10.1080/02786820802178514, 2008.

Barnaba, F., and Gobbi, G. P.: Aerosol seasonal variability over the Mediterranean region and relative impact of maritime, continental and Saharan dust particles over the basin from MODIS data in the year 2001, Atmos. Chem. Phys., 4, 2367–2391, doi:10.5194/acp-4-2367-2004, 2004.

Bonn, B., Bourtsoukidis, E., Sun, T. S., Bingemer, H., Rondo, L., Javed, U., Li, J., Axinte, R., Li, X., Brauers, T., Sonderfeld, H., Koppmann, R., Sogachev, A., Jacobi, S., and Spracklen, D. V.: The link between atmospheric radicals and newly formed particles at a spruce forest site in Germany, Atmos. Chem. Phys., 14, 10823-10843, doi:10.5194/acp-14-10823-2014, 2014.

Borbon, A., Gilman, J. B., Kuster, W. C., Grand, N., Chevaillier, S., Colomb, A., Dolgorouky, C., Gros, V., Lopez, M., Sarda-Esteve, R., Holloway, J., Stutz, J., Perrussel, O., Petetin, H., McKeen, S., Beekmann, M., Warneke, C., Parrishand, D. D., and de Gouw, J. A.: Emission ratios of anthropogenic VOC in northern midlatitude megacities: observations vs. emission inventories in Los Angeles and Paris, J. Geophys. Res., 118, 2041–2057, 2013.

Bryan, A. M., Bertman, S. B., Carroll, M. A., Dusanter, S., Edwards, G. D., Forkel, R., Griffith, S., Guenther, A. B., Hansen, R. F., Helmig, D., Jobson, B. T., Keutsch, F. N., Lefer, B. L., Pressley, S. N., Shepson, P. B., Stevens, P. S., and Steiner, A. L.: In-canopy gas-phase chemistry during CABINEX 2009: sensitivity of a 1-D canopy model to vertical mixing and isoprene chemistry, Atmos. Chem. Phys., 12, 8829-8849, doi:10.5194/acp-12-8829-2012, 2012.

Budisulistiorini, S. H., Li, X., Bairai, S. T., Renfro, J., Liu, Y., Liu, Y. J., McKinney, K. A., Martin, S. T., McNeill, V. F., Pye, H. O. T., Nenes, A., Neff, M. E., Stone, E. A., Mueller, S., Knote, C., Shaw, S. L., Zhang, Z., Gold, A., and Surratt, J. D.: Examining the effects of anthropogenic emissions on isoprene-derived secondary organic aerosol formation during the 2013 Southern Oxidant and Aerosol Study (SOAS) at the Look Rock, Tennessee ground site, Atmos. Chem. Phys., 15, 8871-8888, doi:10.5194/acp-15-8871-2015, 2015.

Capes, G., Murphy, J. G., Reeves, C. E., McQuaid, J. B., Hamilton, J. F., Hopkins, J. R., Crosier, J., Williams, P. I., and Coe, H.: Secondary organic aerosol from biogenic VOCs over West Africa during AMMA, Atmos. Chem. Phys., 9, 3841-3850, doi:10.5194/acp-9-3841-2009, 2009.

Chrit M., Sartelet K., Sciare J., Pey J., Marchand M., Couvidat F., Sellegri K., Beekmann M., 2017. Modelling organic aerosol concentrations and properties during ChArMEx summer campaigns of 2012 and 2013 in the western Mediterranean region. Atm. Chem. Phys. Disc., submitted.

Couvidat, F., Debry, E., Sartelet, K.N., and Seigneur, C.: A hydrophilic/hydrophobic organic (H^2O) aerosol model: Development, evaluation and sensitivity analysis, J. Geophys. Res., 117, D10304, doi:10.1029/2011JD017214, 2012.

Couvidat F., Sartelet K., and Seigneur C.: Investigating the impact of aqueous-phase chemistry and wet deposition on organic aerosol formation using a molecular surrogate modeling approach, Environ. Sci. Tech., 47, 914-922, doi:10.1021/es3034318, 2013.

Couvidat, F., and Sartelet, K.: The Secondary Organic Aerosol Processor (SOAP v1.0) model: a unified model with different ranges of complexity based on the molecular surrogate approach, Geosci. Model Dev., 8, 1111-1138, doi:10.5194/gmd-8-1111-2015, 2015.

Crumeyrolle, S., Schwarzenboeck, A., Roger, J. C., Sellegri, K., Burkhart, J. F., Stohl, A., Gomes, L., Quennehen, B., Roberts, G., Weigel, R., Villani, P., Pichon, J. M., Bourrianne, T., and Laj, P.: Overview of aerosol properties associated with air masses sampled by the ATR-42 during the EUCAARI campaign (2008), Atmos. Chem. Phys., 13, 4877-4893, doi:10.5194/acp-13-4877-2013, 2013.

Day, D. A., Takahama, S., Gilardoni, S., and Russell, L. M.: Organic composition of single and submicron particles in different regions of western North America and the eastern Pacific during INTEX-B 2006, Atmos. Chem. Phys., 9, 5433-5446, doi:10.5194/acp-9-5433-2009, 2009.

Debry, E., Fahey, K., Sartelet, K., Sportisse, B., and Tombette, M.: Technical Note: a new SIze REsolved Aerosol Model (SIREAM), Atmos. Chem. Phys., 7, 1537-1547, doi:10.5194/acp-7-1537-2007, 2007.

DeCarlo, P. F., Dunlea, E. J., Kimmel, J. R., Aiken, A. C., Sueper, D., Crounse, J., Wennberg, P. O., Emmons, L., Shinozuka, Y., Clarke, A., Zhou, J., Tomlinson, J., Collins, D. R., Knapp, D., Weinheimer, A. J., Montzka, D. D., Campos, T., and Jimenez, J. L.: Fast airborne aerosol size and chemistry measurements above Mexico City and Central Mexico during the MILAGRO campaign, Atmos. Chem. Phys., 8, 4027-4048, doi:10.5194/acp-8-4027-2008, 2008.

Ganzeveld, L., Eerdekens, G., Feig, G., Fischer, H., Harder, H., Königstedt, R., Kubistin, D., Martinez, M., Meixner, F. X., Scheeren, H. A., Sinha, V., Taraborrelli, D., Williams, J., Vilà-Guerau de Arellano, J., and Lelieveld, J.: Surface and boundary layer exchanges of volatile organic compounds, nitrogen oxides and ozone during the GABRIEL campaign, Atmos. Chem. Phys., 8, 6223-6243, doi:10.5194/acp-8-6223-2008, 2008.

Gaston, C. J., Riedel, T. P., Zhang, Z., Gold, A., Surratt, J. D., and Thornton, J.A.: Reactive uptake of an isoprene-derived epoxydiol to submicron aerosol particles, Environ. Sci. Technol., 48, 11178–11186, doi:10.1021/es5034266, 2014.

Guenther, A., Karl, T., Harley, P., Wiedinmyer, C., Palmer, P. I., and Geron, C.: Estimates of global terrestrial isoprene emissions using MEGAN (Model of Emissions of Gases and Aerosols from Nature). Atmos. Chem. Phys., 6, 3181–3210, doi:10.5194/acp-6-3181-2006, 2006.

Guenther, A. B., Jiang, X., Heald, C. L., Sakulyanontvittaya, T., Duhl, T., Emmons, L. K., and Wang, X.: The Model of Emissions of Gases and Aerosols from Nature version 2.1 (MEGAN2.1): an extended and updated framework for modeling biogenic emissions, Geosci. Model Dev., 5, 1471–1492, doi:10.5194/gmd-5- 1471-2012, 2012.

Hallquist, M., Wenger, J. C., Baltensperger, U., Rudich, Y., Simpson, D., Claeys, M., Dommen, J., Donahue, N. M., George, C., Goldstein, A. H., Hamilton, J. F., Herrmann, H., Hoffmann, T., Iinuma, Y., Jang, M., Jenkin, M. E., Jimenez, J. L., Kiendler-Scharr, A., Maenhaut, W., McFiggans, G., Mentel, Th. F., Monod, A., Prévôt, A. S. H., Seinfeld, J. H., Surratt, J.

D., Szmigielski, R., and Wildt, J.: The formation, properties and impact of secondary organic aerosol: current and emerging issues, Atmos. Chem. Phys., 9, 5155–5236, doi:10.5194/acp-9-5155-2009, 2009.

Hamilton, J. F., Alfarra, M. R., Robinson, N. Ward, M. W., Lewis, A. C., McFiggans, G. B., Coe, H. and Allan, J. D.: Linking biogenic hydrocarbons to biogenic aerosol in the Borneo rainforest, Atmos. Chem. Phys., 13, 11295–11305, doi: 10.5194/acp-13-11295-2013, 2013.

Held, A., Nowak, A., Birmili, W., Wiedensohler, A., Forkel, R., and Klemm, O., Observations of particle formation and growth in a mountainous forest region in central Europe, J. Geophys. Res. Atmos., 109, D23204, doi:10.1029/2004JD005346, 2004.

Hu, W. W., Campuzano-Jost, P., Palm, B. B., Day, D. A., Ortega, A. M., Hayes, P. L., Krechmer, J. E., Chen, Q., Kuwata, M., Liu, Y. J., de Sá, S. S., McKinney, K., Martin, S. T., Hu, M., Budisulistiorini, S. H., Riva, M., Surratt, J. D., St. Clair, J. M., Isaacman-Van Wertz, G., Yee, L. D., Goldstein, A. H., Carbone, S., Brito, J., Artaxo, P., de Gouw, J. A., Koss, A., Wisthaler, A., Mikoviny, T., Karl, T., Kaser, L., Jud, W., Hansel, A., Docherty, K. S., Alexander, M. L., Robinson, N. H., Coe, H., Allan, J. D., Canagaratna, M. R., Paulot, F., and Jimenez, J. L.: Characterization of a real-time tracer for isoprene epoxydiols-derived secondary organic aerosol (IEPOX-SOA) from aerosol mass spectrometer measurements, Atmos. Chem. Phys., 15, 11807-11833, doi:10.5194/acp-15-11807-2015, 2015.

IPCC: Climate Change 2007: The Physical Science Basis, Intergovernmental Panel for Climate Change Working Group I Rep., Solomon, S., Qin, D., Manning, M., Chen, Z., Marquis, M., Averyt, K. B., Tignor, M., and Miller, H.L. (Eds.), Cambridge University Press, 2007.

Kanawade, V. P., Jobson, B. T., Guenther, A. B., Erupe, M. E., Pressley, S. N., Tripathi, S. N., and Lee, S.-H.: Isoprene suppression of new particle formation in a mixed deciduous forest, Atmos. Chem. Phys., 11, 6013-6027, doi:10.5194/acp-11-6013-2011, 2011.

Kesselmeier, J., and Staudt, M.: Biogenic volatile organic compounds (VOC): An overview on emission,physiology and ecology, J. Atmos. Chem., 33, 23–88, doi:10.1023/A:1006127516791, 1999.

Kiendler-Scharr, A., Wildt, J., Dal Maso, M., Hohaus, T., Kleist, E., Mentel, T. F., Tillmann, R., Uerlings, R., Schurr, U., and Wahner, A.: New particle formation in forests inhibited by isoprene emissions, Nature, 461, 381–384, doi:10.1038/nature08292, 2009.

Krechmer, J. E., Coggon, M. M., Massoli, P., Nguyen, T. B., Crounse, J. D., Hu, W., Day, D. A., Tyndall, G. S., Henze, D. K., Rivera-Rios, J. C., Nowak, J. B., Kimmel, J., Mauldin, R. L., Stark, H., Jayne, J. T., Sipilä, M., Junninen, H., St. Clair, J. M., Zhang, X., Feiner, P. A., Zhang, L., Miller, D. O., Brune, W. H., Keutsch, F. N., Wennberg, P., Seinfeld, J. H., Worsnop, D., Jimenez, J. L., and Canagaratna, M. R.: Formation of low volatility organic compounds and secondary organic aerosol from isoprene hydroxyhydroperoxide low-NO oxidation, Environ. Sci. Tech., 49, 10330-10339, doi: 10.1021/acs.est.5b02031, 2015.

Kulmala, M., Hämeri, K., Mäkelä, J. M., Aalto, P. P., Pirjola, L., Väkevä, M., Nilsson, E. D., Koponen, I. K., Buzorius, G., Keronen, P., Rannik, Ü, Laakso, L., Vesala, T., Bigg, K., Seidl, W., Forkel, R., Hoffmann, T., Spanke, J., Janson, R.,

Shimmo, M., Hansson, H.-C., O'Dowd, C., Becker, E., Paatero, J., Teinilä, K., Hillamo, R., Viisanen, Y., Laaksonen, A., Swietlicki, E., Salm, J., Hari, P., Altimir, N., and Weber, R.: Biogenic aerosol formation in the boreal forest, Boreal Environ. Res., 5, 281–297, 2000.

Kulmala, M., Laakso, L., Lehtinen, K. E. J., Riipinen, I., Dal Maso, M., Anttila, T., Kerminen, V.-M., Hõrrak, U., Vana, M., and Tammet, H.: Initial steps of aerosol growth, Atmos. Chem. Phys., 4, 2553-2560, doi:10.5194/acp-4-2553-2004, 2004.

Laakso, L., Merikanto, J., Vakkari, V., Laakso, H., Kulmala, M., Molefe, M., Kgabi, N., Mabaso, D., Carslaw, K. S., Spracklen, D. V., Lee, L. A., Reddington, C. L., and Kerminen, V.-M. : Boundary layer nucleation as a source of new CCN in savannah environment, Atmos. Chem. Phys., 13, 1957–1972, doi:10.5194/acp-13-1957-2013, 2013.

Lelieveld, J., Butler, T. M., Crowley, J. N., Dillon, T. J., Fischer, H., Ganzeveld, L., Harder, H., Lawrence, M. G., Martinez, M., Taraborrelli, D., and Williams, J.: Atmospheric oxidation capacity sustained by a tropical forest, Nature, 452, 737–740, doi:10.1038/nature06870, 2008.

Loreto, F., Ciccioli, P., Cecinato, A., Brancaleoni, E., Frattoni, M., Fabozzi, C., and Tricoli, D.: Evidence of the photosynthetic origin of monoterpene emitted by Quercus ilex L. leaves by ^{13}C labelling, Plant Physiol., 110, 1317–1322, doi:10.1104/pp.110.4.1317, 1996.

Loÿe-Pilot, M. D., Martin, J. M., and Morelli, J.: Influence of Saharan dust on the rain acidity and atmospheric input to the Mediterranean, Nature, 321, 427-428, doi:10.1038/321427a0, 1986.

Lyamani, H., Olmo, F. J., Alcántara, A., and Alados-Arboledas, L.: Atmospheric aerosols during the 2003 heat wave in southeastern Spain I: Spectral optical depth, Atmos. Environ., 40, 6453–6464. doi:10.1016/j.atmosenv.2006.04.048, 2006.

Mallet, M., Dubovik, O., Nabat, P., Dulac, F., Kahn, R., Sciare, J., Paronis, D., and Léon, J.-F. : Absorption properties of Mediterranean aerosols obtained from multi-year ground-based remote sensing observations, Atmos. Chem. Phys., 13, 9195–9210, doi:10.5194/acp-13-9195-2013, 2013.

Manktelow, P. T., Carslaw, K. S., Mann, G. W., and Spracklen, D. V.: The impact of dust on sulfate aerosol, CN and CCN during an East Asian dust storm, Atmos. Chem. Phys., 10, 365–382, doi:10.5194/acp-10-365-2010, 2010.

Markowicz, K. M., Flatau, P. J., Ramana, M. V., Crutzen, P. J., and Ramanathan, V.: Absorbing Mediterranean aerosols lead to a large reduction in the solar radiation at the surface, Geophys. Res. Lett., 29, 1968. doi:10.1029/2002GL015767, 2002.

Martin, S. T., Andreae, M. O., Artaxo, P., Baumgardner, D., Chen, Q., Goldstein, A. H., Guenther, A., Heald, C. L., Mayol-Bracero, O. L., McMurry, P. H., Pauliquevis,T., Pöschl, U., Prather, K. A., Roberts, G.C., Saleska, S.R., Silva Dias, M. .A., Spracklen, D. V., Swietlicki, E., and Trebs, I.:. Sources and properties of Amazonian aerosol particles, Rev. Geophys., 48, RG2002, doi:10.1029/2008RG000280. 2010.

Middlebrook, A. N., Bahreini, R., Jimenez, J. L., and Canagaratna, M. R.: Evaluation of composition-dependent collection efficiencies for the Aerodyne aerosol mass spectrometer using field data, Aerosol Sci. Tech, 46, 258–271, doi:10.1080/02786826.2011.620041, 2012.

Nedelec, P, Cammas, J.-P., Thouret, V., Athier, G., Cousin, J.-M., Legrand, C., Abonnel, C., Lecoeur, F., Cayez, G., and Marizy, C.: An improved infrared carbon monoxide analyser for routine measurements aboard commercial Airbus aircraft:

technical validation and first scientific results of the MOZAIC III programme, Atmos. Chem. Phys., 3, 1551-1564, doi:10.5194/acp-3-1551-2003, 2003.

Nenes, A., Pandis, S. N., and Pilinis, C.: ISORROPIA: A new thermodynamic equilibrium model for multiphase multicomponent inorganic aerosols, Aquat. Geochem., 4, 123–152, doi:10.1023/A:1009604003981, 1998.

Nguyen, T. B., Coggon, M. M., Bates, K. H., Zhang, X., Schwantes, R. H., Schilling, K. A., Loza, C. L., Flagan, R. C., Wennberg, P. O., and Seinfeld, J. H.: Organic aerosol formation from the reactive uptake of isoprene epoxydiols (IEPOX) onto non-acidified inorganic seeds, Atmos. Chem. Phys., 14, 3497-3510, doi:10.5194/acp-14-3497-2014, 2014.

Papadimas, C. D., Hatzianastassiou, N., Matsoukas, C., Kanakidou, M., Mihalopoulos, N., and Vardavas, I.: The direct effect of aerosols on solar radiation over the broader Mediterranean basin, Atmos. Chem. Phys., 12, 7165-7185, doi:10.5194/acp-12-7165-2012, 2012.

Raatikainen, T., Vaattovaara, P., Tiitta, P., Miettinen, P., Rautiainen, J., Ehn, M., Kulmala, M., Laaksonen, A., and Worsnop, D. R.: Physicochemical properties and origin of organic groups detected in boreal forest using an aerosol mass spectrometer, Atmos. Chem. Phys., 10, 2063-2077, doi:10.5194/acp-10-2063-2010, 2010.

Riva, M., Bell, D. M., Kaldal Hansen, A.-M., Drozd, G. T., Zhang, Z., Gold, A., Imre, D., Surratt, J. D., Glasius, M., and Zelenyuk, A.: Effect of organic coatings, humidity and aerosol acidity on multiphase chemistry of isoprene epoxydiols, Environ. Sci. Technol. 50, 5580–5588, doi:10.1021/acs.est.5b06050, 2016.

Robinson, N. H., Hamilton, J. F., Allan, J. D., Langford, B., Oram, D. E., Chen, Q., Docherty, K., Farmer, D. K., Jimenez, J. L., Ward, M. W., Hewitt, C. N., Barley, M. H., Jenkin, M. E., Rickard, A. R., Martin, S. T., McFiggans, G., and Coe, H.: Evidence for a significant proportion of Secondary Organic Aerosol from isoprene above a maritime tropical forest, Atmos. Chem. Phys., 11, 1039-1050, doi:10.5194/acp-11-1039-2011, 2011.

Sartelet, K. N., Couvidat, F., Seigneur, C., and Roustan, Y.: Impact of biogenic emissions on air quality over Europe and North America, Atmos. Environ., 53, 131–141, doi:10.1016/j.atmosenv.2011.10.046, 2012.

Schwartz, R. E., Russell, L. M., Sjostedt, S. J., Vlasenko, A., Slowik, J. G., Abbatt, J. P. D., Macdonald, A. M., Li, S. M., Liggio, J., Toom-Sauntry, D., and Leaitch, W. R.: Biogenic oxidized organic functional groups in aerosol particles from a mountain forest site and their similarities to laboratory chamber products, Atmos. Chem. Phys., 10, 5075-5088, doi:10.5194/acp-10-5075-2010, 2010.

Sciare, J., Bardouki, H., Moulin, C., and Mihalopoulos, N.: Aerosol sources and their contribution to the chemical composition of aerosols in the Eastern Mediterranean Sea during summertime, Atmos. Chem. Phys., 3, 291-302, doi:10.5194/acp-3-291-2003, 2003.

Setyan, A., Song, C., Merkel, M., Knighton, W. B., Onasch, T. B., Canagaratna, M. R., Worsnop, D. R., Wiedensohler, A., Shilling, J. E., and Zhang, Q.: Chemistry of new particle growth in mixed urban and biogenic emissions – insights from CARES, Atmos. Chem. Phys., 14, 6477-6494, doi:10.5194/acp-14-6477-2014, 2014.

Shilling, J. E., Zaveri, R. A., Fast, J. D., Kleinman, L., Alexander, M. L., Canagaratna, M. R., Fortner, E., Hubbe, J. M., Jayne, J. T., Sedlacek, A., Setyan, A., Springston, S., Worsnop, D. R., and Zhang, Q.: Enhanced SOA formation from mixed

anthropogenic and biogenic emissions during the CARES campaign, Atmos. Chem. Phys., 13, 2091-2113, doi:10.5194/acp-13-2091-2013, 2013..

Sihto, S.-L., Kulmala, M., Kerminen, V.-M., Dal Maso, M., Petäjä, T., Riipinen, I., Korhonen, H., Arnold, F., Janson, R., Boy, M., Laaksonen, A., and Lehtinen, K. E. J.: Atmospheric sulphuric acid and aerosol formation: implications from atmospheric measurements for nucleation and early growth mechanisms, Atmos. Chem. Phys., 6, 4079-4091, doi:10.5194/acp-6-4079-2006, 2006.

Slowik, J. G., Slowik, J. G., Stroud, C., Bottenheim, J. W., Brickell, P. C., Chang, R. Y.-W., Liggio, J., Makar, P. A., Martin, R. V., Moran, M. D., Shantz, N. C., Sjostedt, S. J., van Donkelaar, A., Vlasenko, A., Wiebe, H. A., Xia, A. G., Zhang, J., Leaitch, W. R., and Abbatt, J. P. D.: Characterization of a large biogenic secondary organic aerosol event from eastern Canadian forests, Atmos. Chem. Phys., 10, 2825-2845, doi:10.5194/acp-10-2825-2010, 2010.

Spracklen, D. V., Bonn, B., and Carslaw, K. S.: Boreal forests, aerosols and the impacts on clouds and climate, Philos. Trans. R. Soc. Lond. A, 366, 4613–4626, doi:10.1098/rsta.2008.0201, 2008.

Ulbrich, I. M., Canagaratna, M. R., Zhang, Q., Worsnop, D. R., and Jimenez, J. L.: Interpretation of organic components from positive Matrix Factorization of aerosol mass spectrometric data, Atmos. Chem. Phys., 9, 2891-2918, doi:10.5194/acp-9-2891-2009, 2009.

Zhang Y., L. Tang, Y. Sun , O. Favez , F.Canonaco, A.Albinet3 , F. Couvidat, D. Liu7 , J. T. Jayne, Z. Wang, P. L. Croteau, M. R. Canagaratna, H.-C. Zhou, A. S. H. Prévôt and D. R. Worsnop. Limited formation of isoprene epoxydiols-derived secondary organic aerosol under NOx-rich environments in Eastern China, Geophys. Res. Lett., 44,2035–2043, doi:10.1002/2016GL072368.

Atmos. Chem. Phys. Discuss., https://doi.org/10.5194/acp-2017-482
Manuscript under review for journal Atmos. Chem. Phys.
Discussion started: 18 July 2017

Atmospheric Chemistry and Physics Discussions

Table 1. Concentrations of the different gas phase species (ppbV) measured aboard each flight.

Flight	dd/mm (2014)	Isoprene	MVK+ MACR+ ISOPOOH	Monoterpenes	Toluene	Benzene	O_3	CO	NO_W	NO
RF15	30/06	583±290	214±91	117±82	146±59	93±61	40±8.8	118±27	4.2±0.8	0.17±0.3
RF 20	03/07	1240±527	756±287	205±107	149±82	102±42	53±4.0	136±46	7.9±2.3	0.31±0.2
RF 21	05/07	600±262	365±182	179±128	147±176	108 ±53	31±8.0	79±11	5.86±0.7	0.29±0.3
RF 23	07/07	392±197	230±159	119±87	74±34	88 ±18	52±3.0	88±9	5.6±2.1	0.29±0.9

Table 2. Concentrations of the different chemical species measured aboard each flight during level low altitude legs.

Flight	dd/mm (2014)	NR-PM1	Org	SO4	NO3	BC
RF15	30/06	0.70±0.08	0.48±0.23	0.08±0.07	0.013±0.01	0.03±0.02
RF 20	03/07	2.70±1.10	1.79±0.70	0.48±0.2	0.10±0.06	0.11±0.03
RF 21	05/07	0.99±0.50	0.72±0.40	0.20±0.09	0.03±0.02	0.11±0.04
RF 23	07/07	1.64±0.70	0.96±0.60	0.30±0.18	0.06±0.07	0.08±0.06

Table 3: Correlations for different time series during RF 20 03/07 and RF 23 07/07.

	MOOA		**LOOA**	
	RF 20 03/07	**RF 23 07/07**	**RF 20 03/07**	**RF 23 07/07**
	Pr (n =91)	Pr (n= 144)	Pr (n =91)	Pr (n =169)
PTR-MS m/z 69 (Isoprene)	0.11	0.41	0.51	0.67
PTR-MS m/z 71 (MVK+MCR+ISOPOOH)	0	0.28	0.64	0.71
PTR-MS m/z 137	0.59	0.58	0.29	0.49
PTR-MS m/z 93	0.15	0.25	0.27	0.38
PTR-MS m/z 79	0.04	0.21	0	0.15
BC	0.52	0.48	0.61	0.48
CO	0.37	0.48	0.34	0.60
NO_W	0.56	0.44	0.51	0.60

Atmos. Chem. Phys. Discuss., https://doi.org/10.5194/acp-2017-482
Manuscript under review for journal Atmos. Chem. Phys.
Discussion started: 18 July 2017

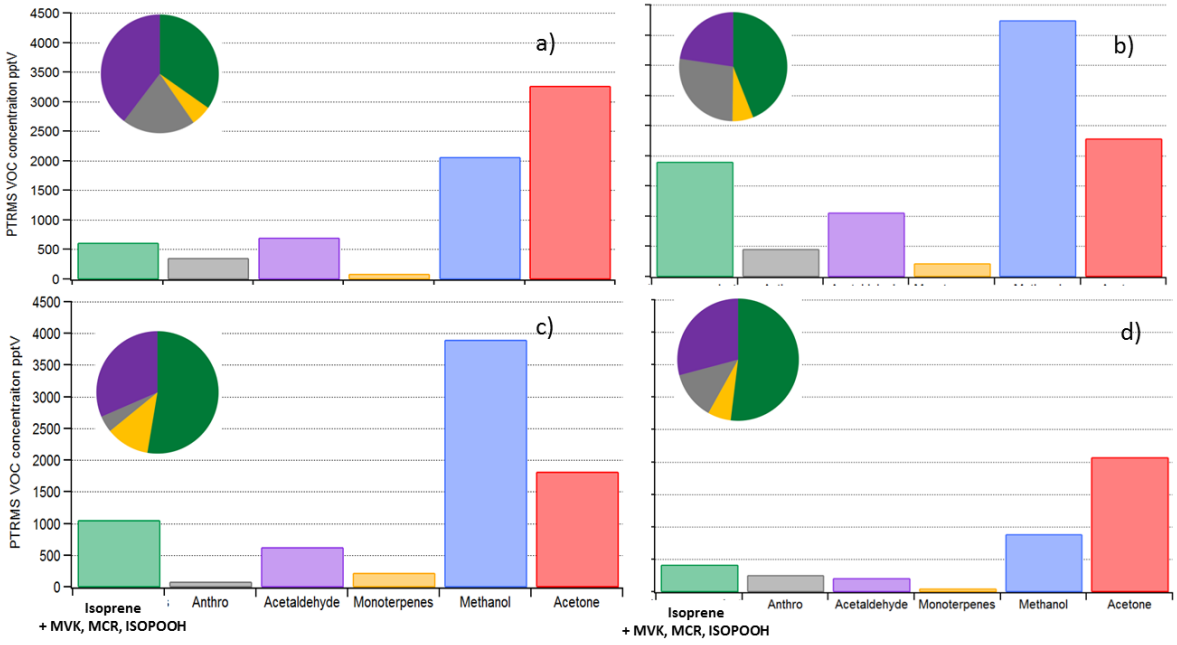

Figure 1. Contribution of the different measured gas phase species aboard the ATR-42: a) RF15 3006, b) RF20 0307, c) RF21 0507, d) RF23 0707. The pie charts illustrated in each figure represent the contribution of all VOC species *except those of methanol and acetone*.

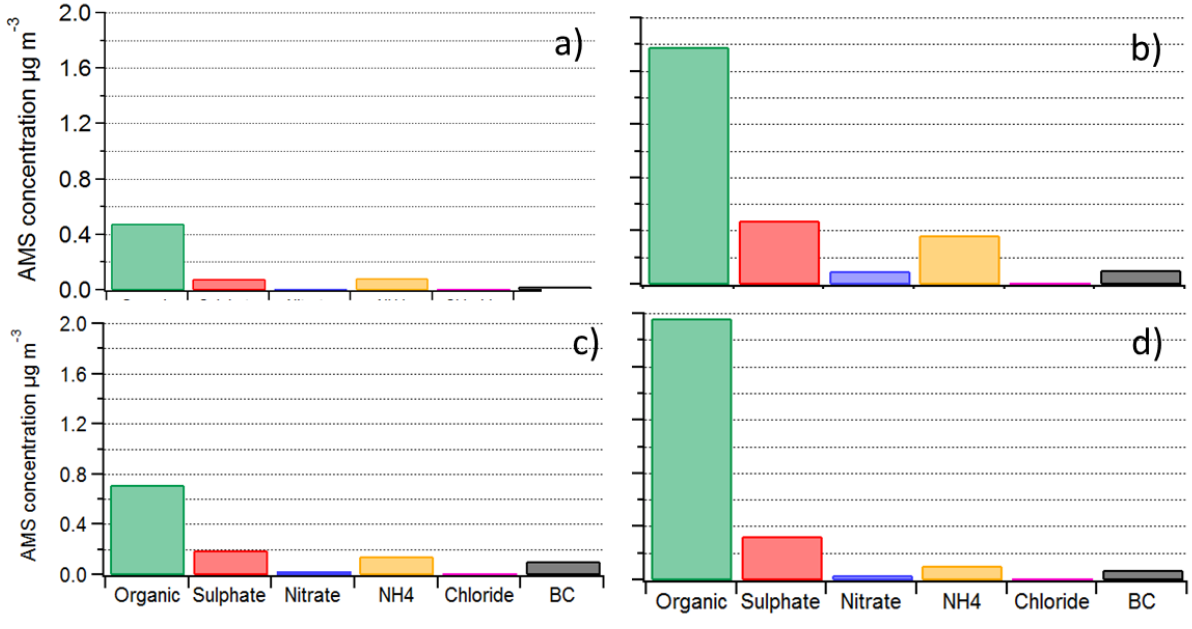

Figure 2. Contribution of the non-refractory aerosol chemical species aboard the ATR-42: a) RF15 3006 b) RF20 0307, c) RF21 0507, d) RF23 0707.

Atmos. Chem. Phys. Discuss., https://doi.org/10.5194/acp-2017-482
Manuscript under review for journal Atmos. Chem. Phys.
Discussion started: 18 July 2017

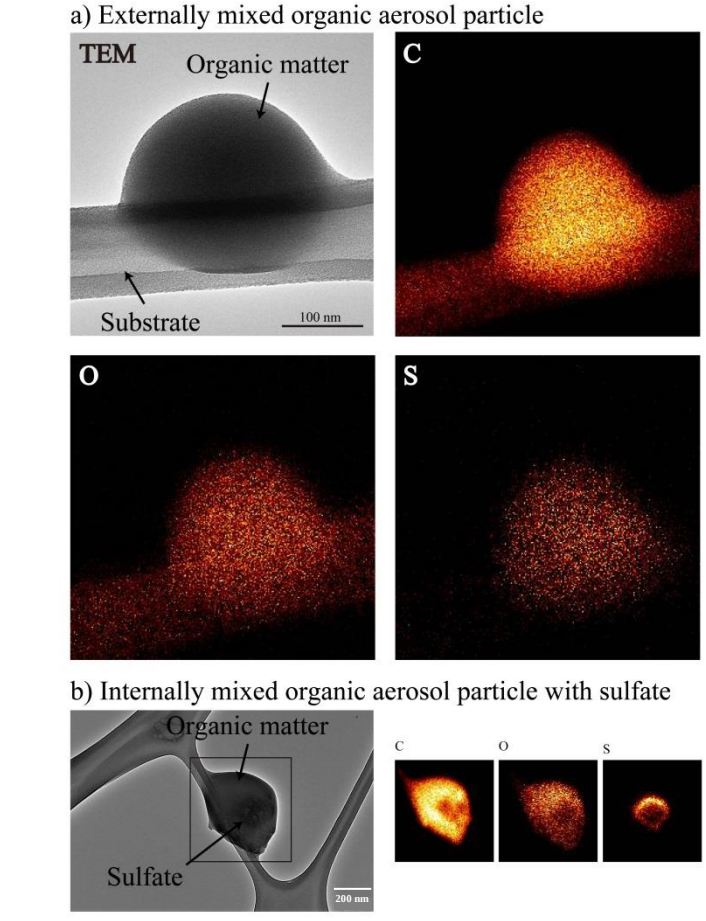

Figure 3. a) Example of an externally mixed organic aerosol particle showing signals of S; b) Internally mixed organic and ammonium sulphate aerosols.

Atmos. Chem. Phys. Discuss., https://doi.org/10.5194/acp-2017-482
Manuscript under review for journal Atmos. Chem. Phys.
Discussion started: 18 July 2017

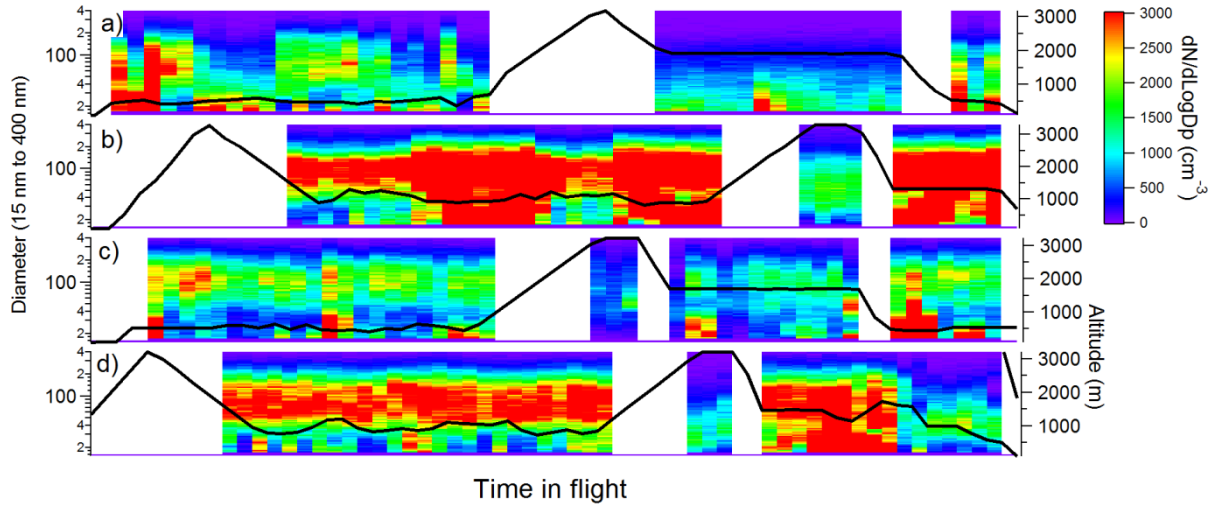

Figure 4. Aerosol size distribution measured by the SMPS for a) RF15 3006 b) RF20 0307, c) RF21 0507, d) RF23 0307. The colour scale indicates aerosol concentration dN/dlogDp. Altitude is illustrated as the black line and is represented on the right hand axis.

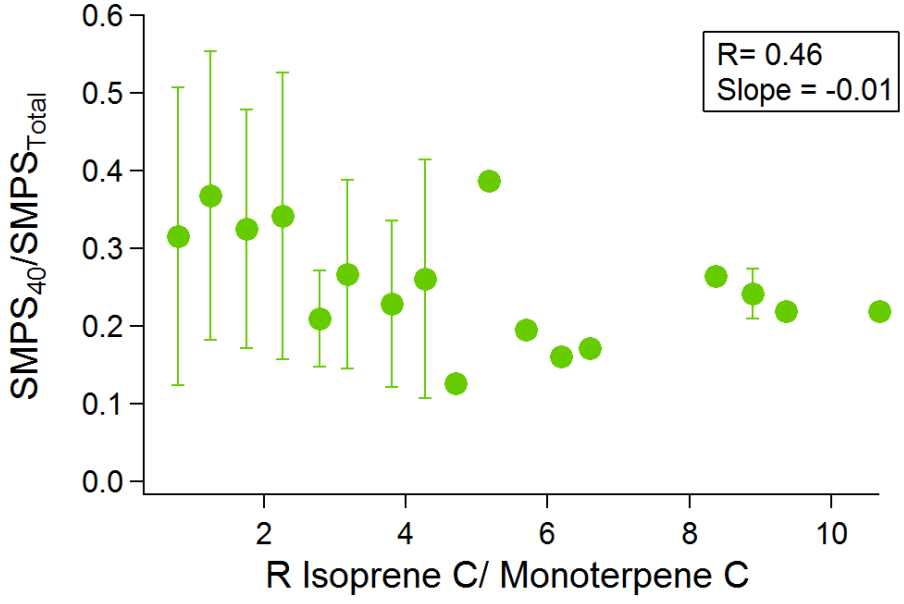

Figure 5. Ratios of IsopreneC/MonoterpeneC plotted as a function of F40, averaged for the four 'biogenic' flights. Error bars represent ± 1 σ.

Atmos. Chem. Phys. Discuss., https://doi.org/10.5194/acp-2017-482
Manuscript under review for journal Atmos. Chem. Phys.
Discussion started: 18 July 2017

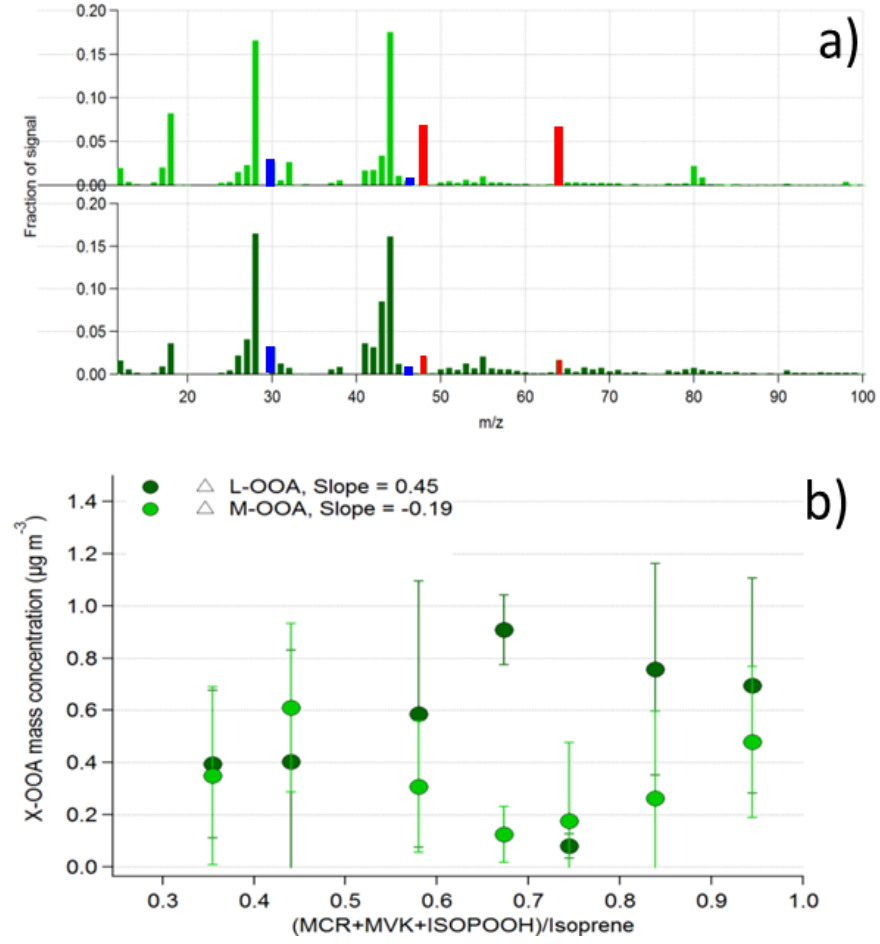

Figure 6. a) A two factor solution determined from PMF analysis of the biogenic research flights. The more oxidised organic aerosol (MOOA) associated with inorganic peaks for sulphate and nitrate, the less oxidised organic aerosol (LOOA) with a lower contribution of inorganic peaks. b) Variations of these two species with photochemical age of airmass.

Atmos. Chem. Phys. Discuss., https://doi.org/10.5194/acp-2017-482
Manuscript under review for journal Atmos. Chem. Phys.
Discussion started: 18 July 2017

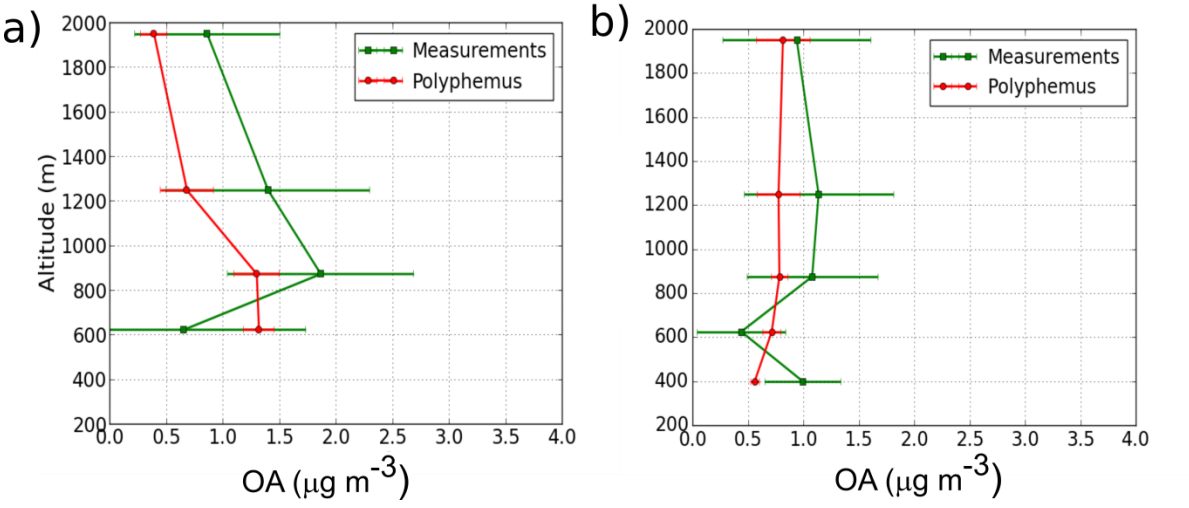

Figure 7. Measured (green) and modelled (red) organic concentrations during the a) RF20 03/07 and the b) RF23 07/07 flights. The concentrations are averaged on the vertical layers of the model in the vertical and variations around the average are indicated by the horizontal bars.

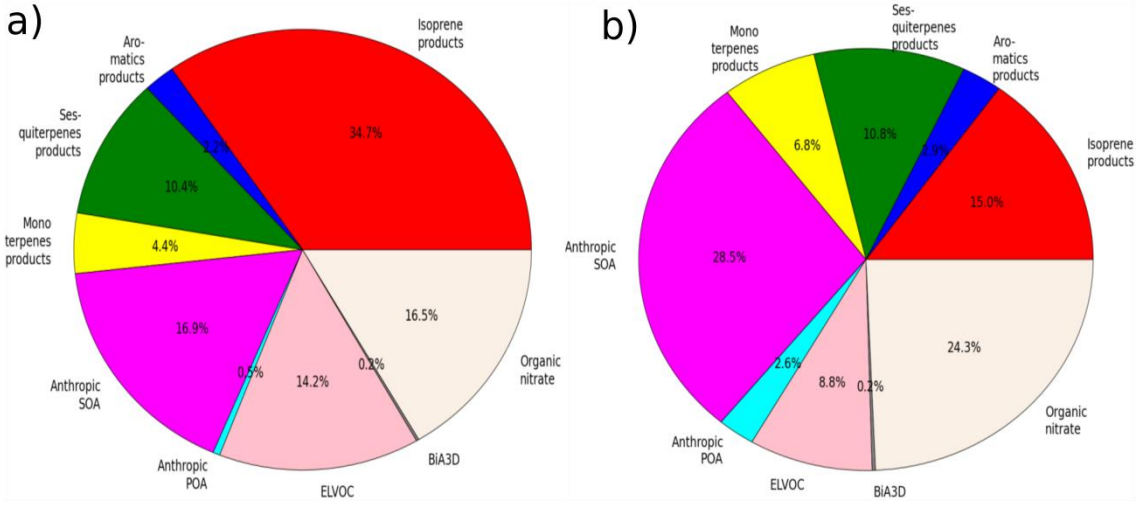

Figure 8: Modelled averaged composition of OA_1 along the flight path during the a) RF20 03/07 and the b) RF23 07/07 flights. This averaged composition is obtained by averaging concentrations along the flight path at altitudes below 1000m.